High-capacity iodine adsorption and nonporous to porous structural transformation in an originally nonporous coordination polymer

Chu-Hong Zhang, Bing-Xun Zhou, Xian Lin, Jia-Xuan Wu, Liang-Hua Wu, Songliang Cai, Jun Fan, Wei--Guang Zhang,* Yong Yan,* and Sheng-Run Zheng*

GDMPA Key Laboratory for Process Control and Quality Evaluation of Chiral Pharmaceuticals, and Guangzhou Key Laboratory of Analytical Chemistry for Biomedicine, School of Chemistry, South China Normal University, Guangzhou 510006, P. R. China

*Corresponding author: Dr. Sheng-Run, Zheng; Dr. Wei-Guang Zhang; Yong Yan

E-mail address: zhengsr@scnu.edu.cn; wgzhang@scnu.edu.cn; Yong.Yan@m.scnu.edu.cn

Tel./Fax. : +86-20-39310187

Supporting Information

EXPERIMENTAL SECTION

Materials and instruments

All reagents of analytical grade were purchased from Guangzhou Chemical Reagent Factory and used without further purification. IR spectra were recorded using a Nicolet FT-IR -170SX spectrometer in the region of 4000-400 cm^{-1} using KBr pellets. Powder X-ray diffraction (PXRD) was carried out with an Ultima IV X-ray powder diffractometer (Kurary, Tokyo, Japan) at 40 kV and 40 mA using Cu K_α radiation (k = 1.5406 Å). Element content was recorded in an Elemental Vario Microcube. X-ray single-crystal diffraction data were collected on a Bruker D8 Venture. Thermogravimetric analysis (TGA) was performed on a NETZSCH TG209 system in a flowing air atmosphere at a heating rate of 10 °C min^{-1}. ^1H NMR spectra were recorded on a Bruker AVANCE NEO spectrometer (600 MHz). The N_2 adsorption-desorption isotherms were taken on a Micromeritics 3Flex adsorption instrument. Raman spectroscopy measurements were performed on a Renishaw inVia Reflex Raman spectrometer with a laser radiation line at 785 nm. X-ray

photoelectron spectra (XPS) were recorded on a Shimadzu AXIS SUPRA X-ray photoelectron spectrometer. Inductively coupled plasma (ICP) data were obtained on an Agilent ICP–OES730. EDS images were recorded on a ZEISS Gemini 500 scanning electron microscope at 15.0 kV. Micromorphology images were obtained by a FEITalosF200X transmission electron microscope.

Synthesis of 4,4'-(4-(4-(1H-imidazol-1-yl)phenyl)pyridine-2,6-diyl)dibenzoic acid (H_2IPDA)

H_2IPDA was successfully synthesized through three steps. In the first step, referring to the Buchwald-Hartwig reaction, a mixture of imidazole (3.4 g, 0.05 mol), K_2CO_3 (5.0 g, 36 mmol), 4-fluorobenzaldehyde (5.4 mL, 0.05 mmol), N,N-dimethylformamide (DMF, 30 mL), and Aliquat336 (2.6 g, 6 mmol) was added to a three-neck flask, heated and refluxed at 120 °C for 24 hours. When cooled to room temperature, 150 mL of ice water was added, and a yellow solid was precipitated from the solution. The yellow solid was filtered and dried to obtain 4-(1-H-imidazole-1-yl) benzaldehyde.

In the second step, 4-(1-H-imidazol-1-yl) benzaldehyde (3.44 g, 20 mmol) was added to an EtOH (200 mL) solution of NaOH (1.6 g, 40 mmol) and *p*-cyanophenone (5.8 g, 40 mmol). The reaction was carried out at room temperature for 24 hours, followed by the addition of ammonia (80 mL, 25%) for 48 hours to form a light-yellow precipitate. Further filtration, washing, and drying were carried out to obtain 4,4'-(4-(4-(1H-imidazol-1-yl)phenyl)pyridine-2,6-diyl)dibenzonitrile (IPD).

The third step was to add IPD (2.0 g, 4.7 mmol) to the aqueous solution of KOH (0.78 g, 14 mmol), homogenize it by ultrasonication, heat it at 150 °C in a stainless steel high pressure tank lined with polytetrafluoroethylene for 48 hours, cool to room temperature, form a yellowish clarification solution, add hydrochloric acid (1 M, 5 mL), filter the precipitate, and obtain the desired product 4-(4-(1H-imidazol-1-yl) phenyl) pyridine-2pyrrolic acid (H_2IPDA) in 63% yield. ^{1}H NMR (600 MHz, DMSO-d_6): δ 8.51-8.46 (m, 4H), 8.44 (t, J = 1.2 Hz, 1H), 8.41 (s, 2H), 8.28 -8.25 (m, 2H), 8.13-8.09 (m, 4H), 7.91 (t, J = 1.4 Hz, 1H), 7.90-7.87 (m, 2H), 7.16 (t, J = 1.1 Hz, 1H). IR (KBr，cm^{-1}): 3131(s), 2768(w), 2468(w), 1708(s), 1598(s), 1530(s), 1390(s), 1310(w), 1238(s), 1112(m), 1060(m), 830(s), 778(s), 516(m).

Adsorption of organic dyes

The adsorption properties of Zn-IPDA and I_2@Zn-IPDA-100%-rel for methylene blue (MLB), crystal violet (CV), rhodamine B (RhB) and Congo red (CR) were studied. At room temperature, Zn-IPDA (10 mg) and I_2@Zn-IPDA-100%-rel (10 mg) were added to a 20 ppm (MLB, CV, RhB) or 100 ppm (CR) organic dye aqueous solution (15 mL), respectively. Within a given time, approximately 3 mL of the solution was taken out with a syringe and filtered, and the dye concentration was determined using a UV Vis spectrometer.

X-ray Data Collection and Structure Refinement

Data collection was recorded at 296 K on a Bruker APEX-II CCD with a graphite monochromated Mo X-ray source (λ = 0.71073 Å) for Co-IPT-IBA. Multiscan empirical absorption correction was applied by using SADABS. The olex2.solve[S1] and SHELXL-2016[S2] program packages were used for the structural solutions and refinements based on F^2, respectively. All non-H atoms were refined with anisotropic thermal parameters. Hydrogen atoms, except for water molecules and OH^-, were generated according to their idealized positions and refined isotropically. The hydrogen atoms on the coordinated water molecule and OH^- were not added based but included in the formula. The contributions of disordered solvent molecules in the micropores were removed by SQUEEZE. [S3] Table S1 contains the details for the crystal parameters, data collection, and refinement. Selected bond lengths and angles are provided in Table S2. The CCDC reference number is 2268979.

Theoretical Calculation Methods

The Gaussian 16 suite of programs[S4] was used to optimize the configurations. The binding energies were determined using the b3lyp functional with the def2svp basis set corrected for superposition error (BSSE).

EXAFS Analysis

Data reduction, data analysis, and EXAFS fitting were performed and analysed with the Athena and Artemis programs of the Demeter data analysis packages[S5] that utilize the FEFF6 program[S6] to fit the EXAFS data. The energy calibration of the sample was conducted through a standard and Zn foil, which was simultaneously measured as a reference. A linear function was subtracted from the preedge region, and then the edge jump was normalized using Athena software. The χ(k) data were isolated by subtracting a smooth, third-order polynomial approximating the absorption background of an isolated atom. The *k3*-weighted *χ(k)* data were Fourier transformed after applying a HanZnng window function (*Δk* = 1.0). For EXAFS modelling, the global amplitude EXAFS (*CN, R,* σ^2 and ΔE_0) was obtained by nonlinear fitting, with least-squares refinement, of the EXAFS equation to the Fourier transformed data in *R*-space using Artemis software. The EXAFS of the Zn foil was fitted, and the obtained amplitude reduction factor S_0^2 value (1.00) was set in the EXAFS analysis to determine the coordination numbers (*CNs*) in the Zn-O, Zn-N, Zn-I scattering path in the sample.

Scheme S1. Synthesis of H_2IPDA.

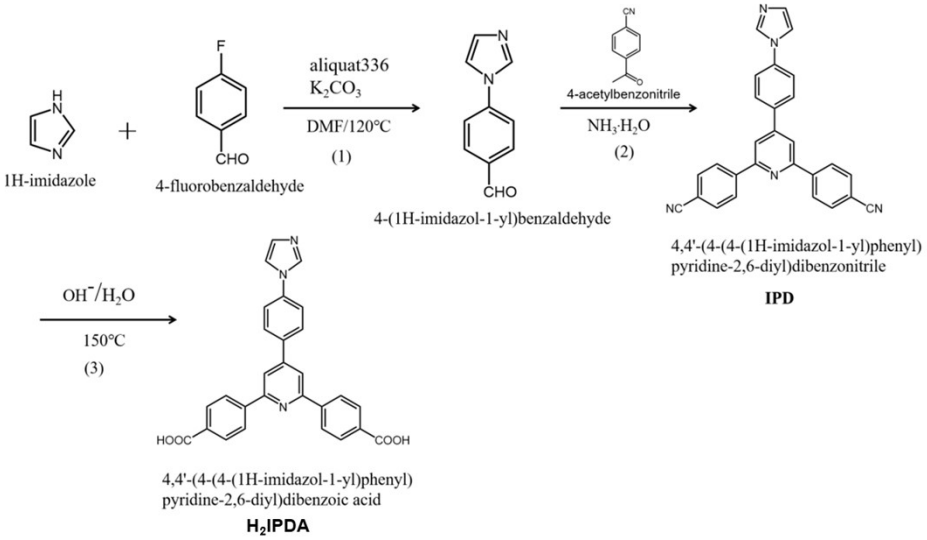

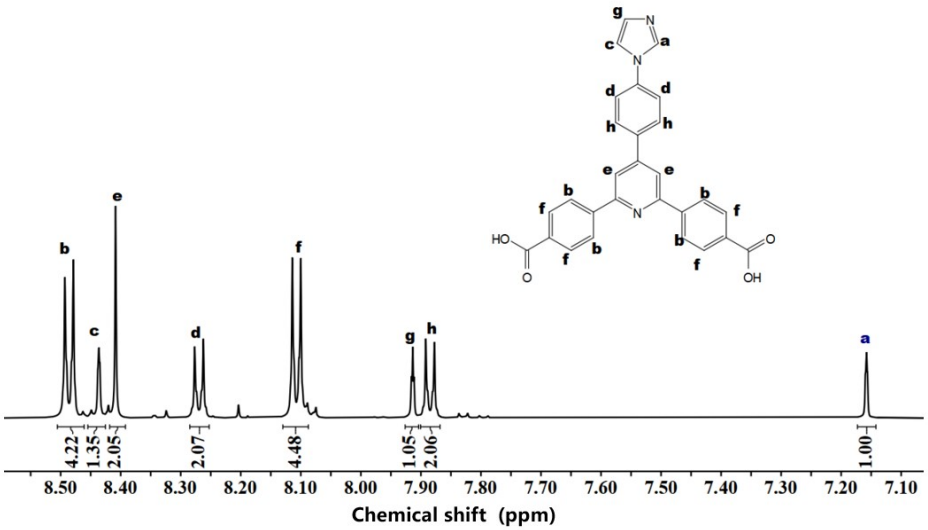

Fig. S1 ^{1}H NMR spectrum (600 MHz, 298 K, DMSO-d_6) of H_2IPDA.

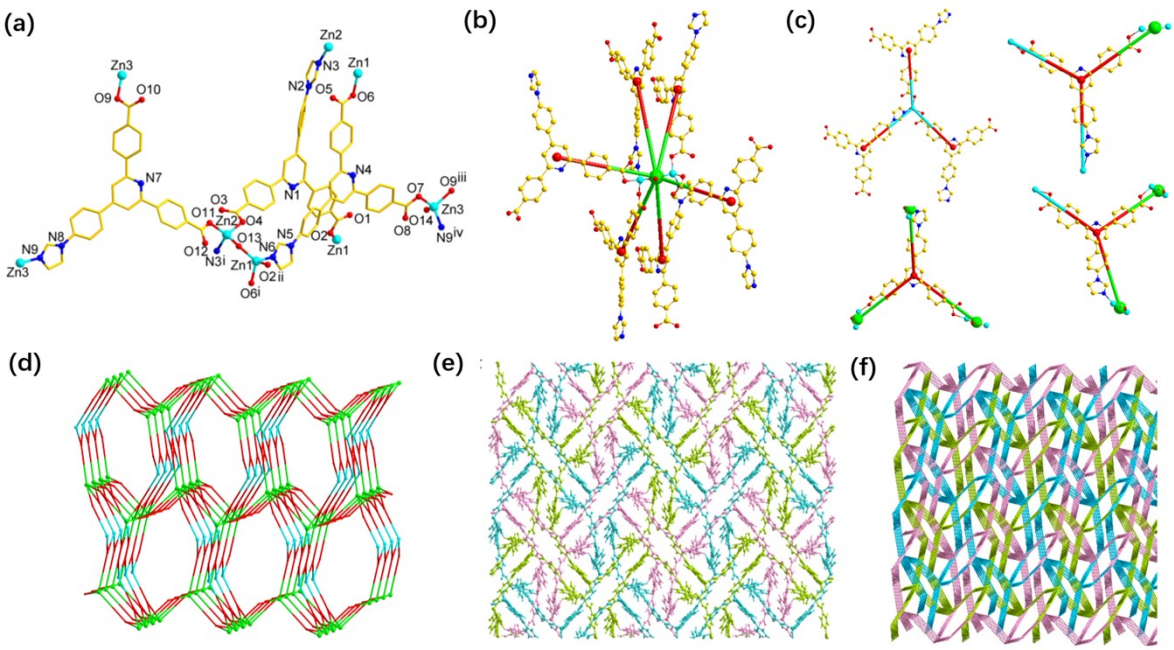

Fig. S2 (a) The coordination environment of Zn(II) and coordination mode of ligands in Zn-IPDA. Symmetric codes: (i) -1 +x, y, z; (ii) -1/2 + x, 3/2 -y, -1/2 + z; (iii) 5/2 – x, 3/2 + y, 1/2 – z; (iv) 3/2 – x, 3/2 + y, 1/2 – z. (b) The six-connected node in Zn-IPDA. (c) The three connected nodes in Zn-IPDA. (d) The (3,6)-connected network topology in Zn-IPDA. (e) Th three-folded interpenetrated framework in Zn-IPDA. (f) The three-folded interpenetrating network topology in Zn-IPDA.

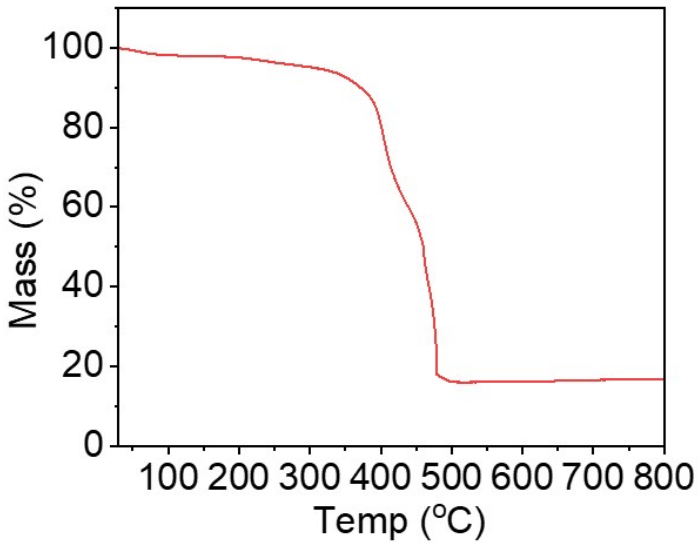

Fig. S3 TG curve of the as-synthesized Zn-IPDA.

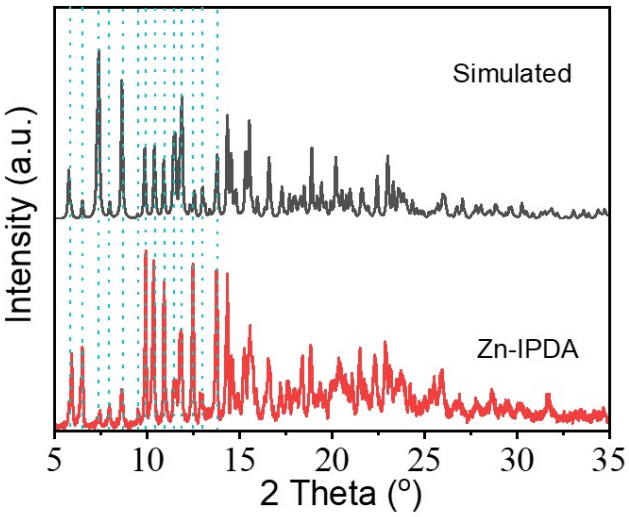

Fig. S4 PXRD of the simulated and as-synthesized Zn-IPDA.

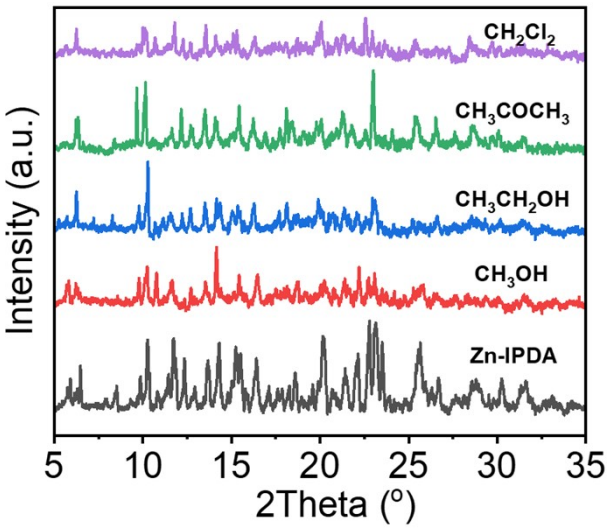

Fig. S5 PXRD of Zn-IPDA before and after immersion in selected organic solvents for 72 h.

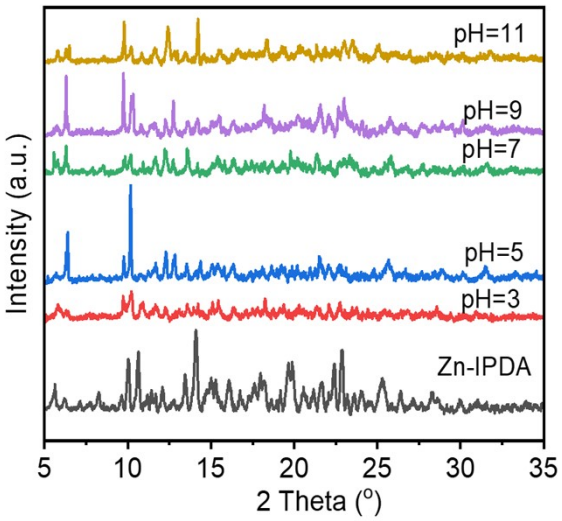

Fig. S6 PXRD of Zn-IPDA before and after immersion in aqueous solutions with different pH values for 72 h.

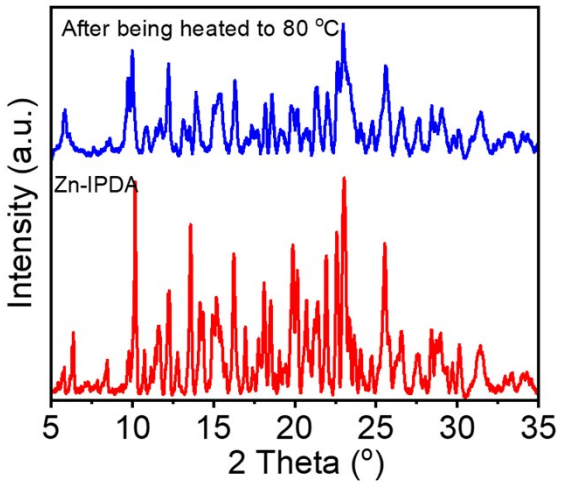

Fig. S7 PXRD of Zn-IPDA before and after heating at 80 °C.

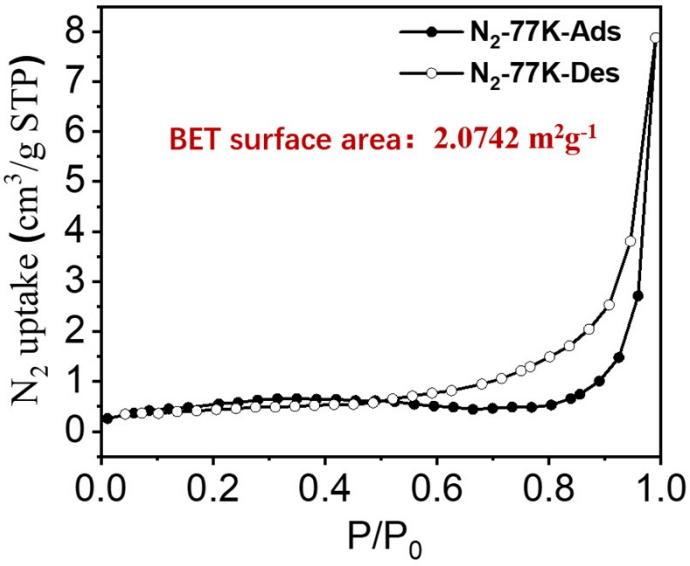

Fig. S8 N_2 adsorption-desorption isomer of Zn-IPDA at 77 K.

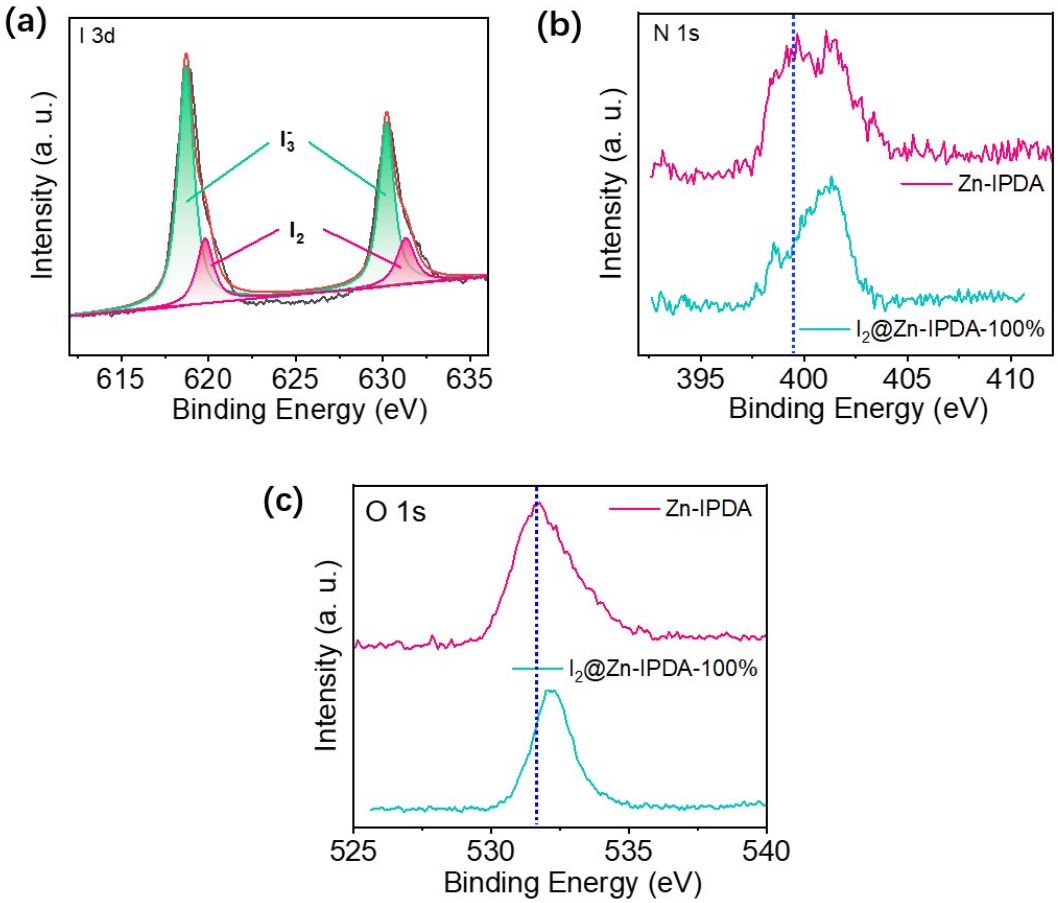

Fig. S9 (a) The I 3d XPS spectrum of I_2@Zn-IPDA-100%. The (b) N 1 s and (c) O 1 s XPS spectra of Zn-IPDA and I_2@Zn-IPDA-100%.

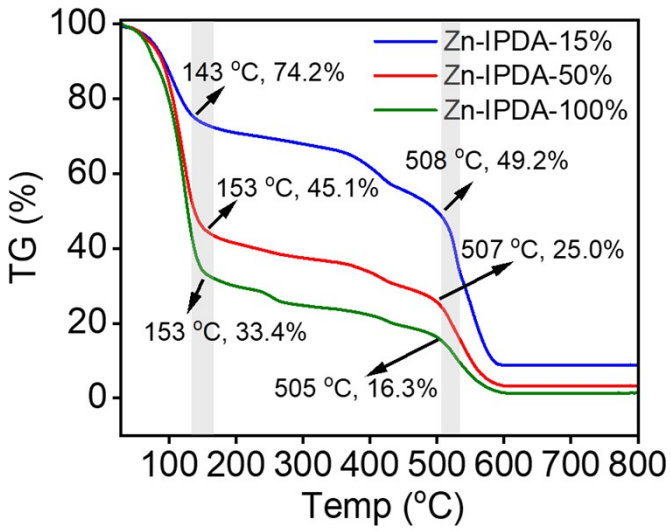

Fig. S10 TG curves of I_2@Zn-IPDA-15%, I_2@Zn-IPDA-50%, and I_2@Zn-IPDA-100%.

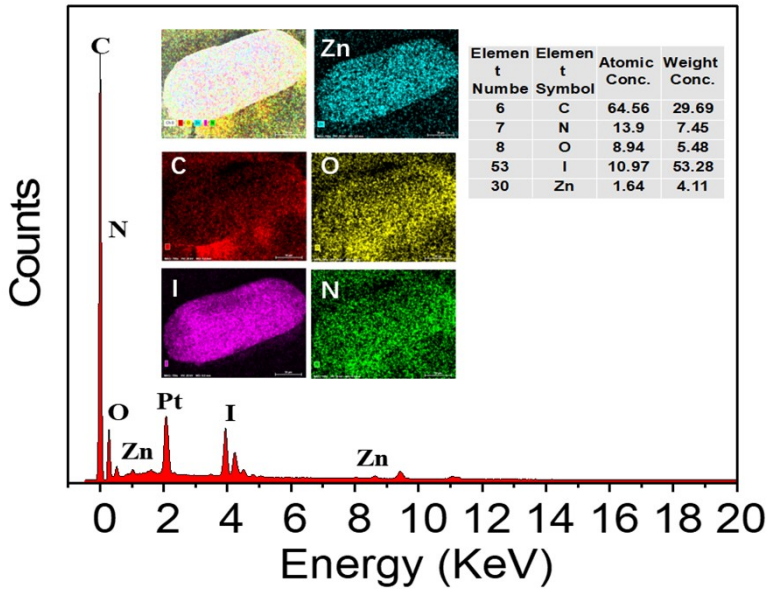

Fig. S11 EDS and mapping of I_2@Zn-IPDA-100%.

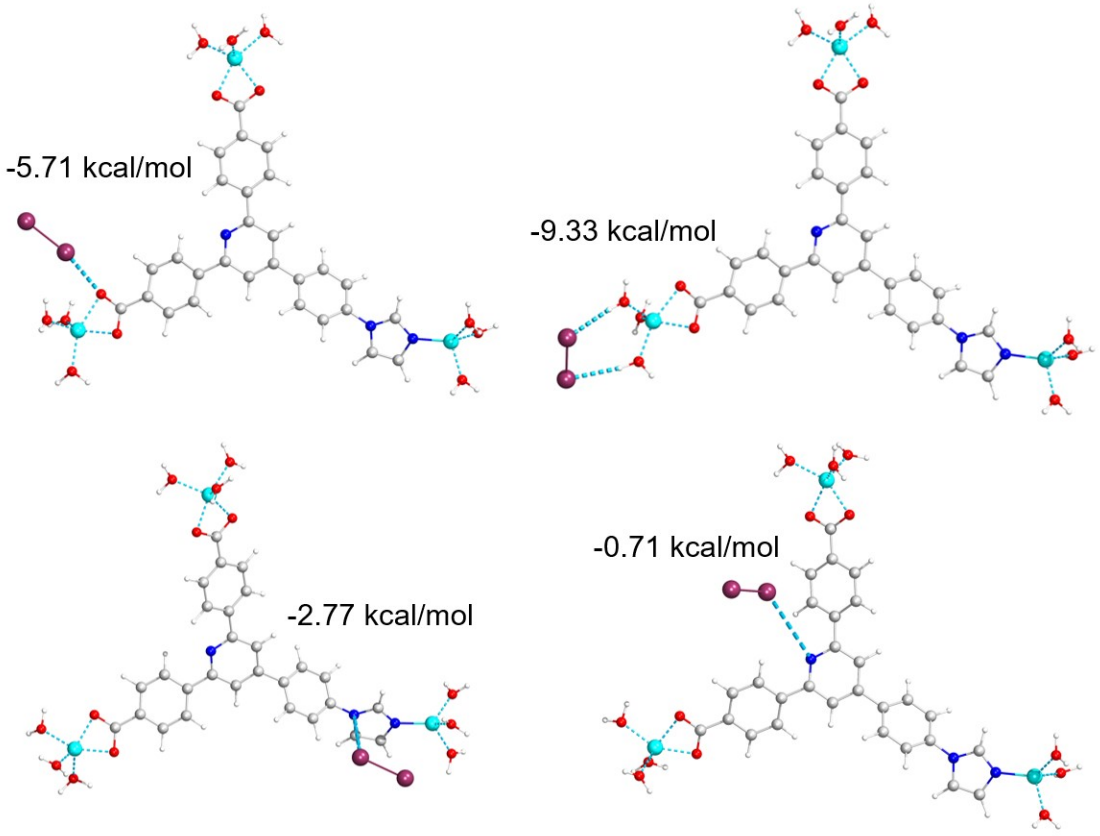

Fig. S12 DFT calculation results of the binding energy between iodine molecules and different sites.

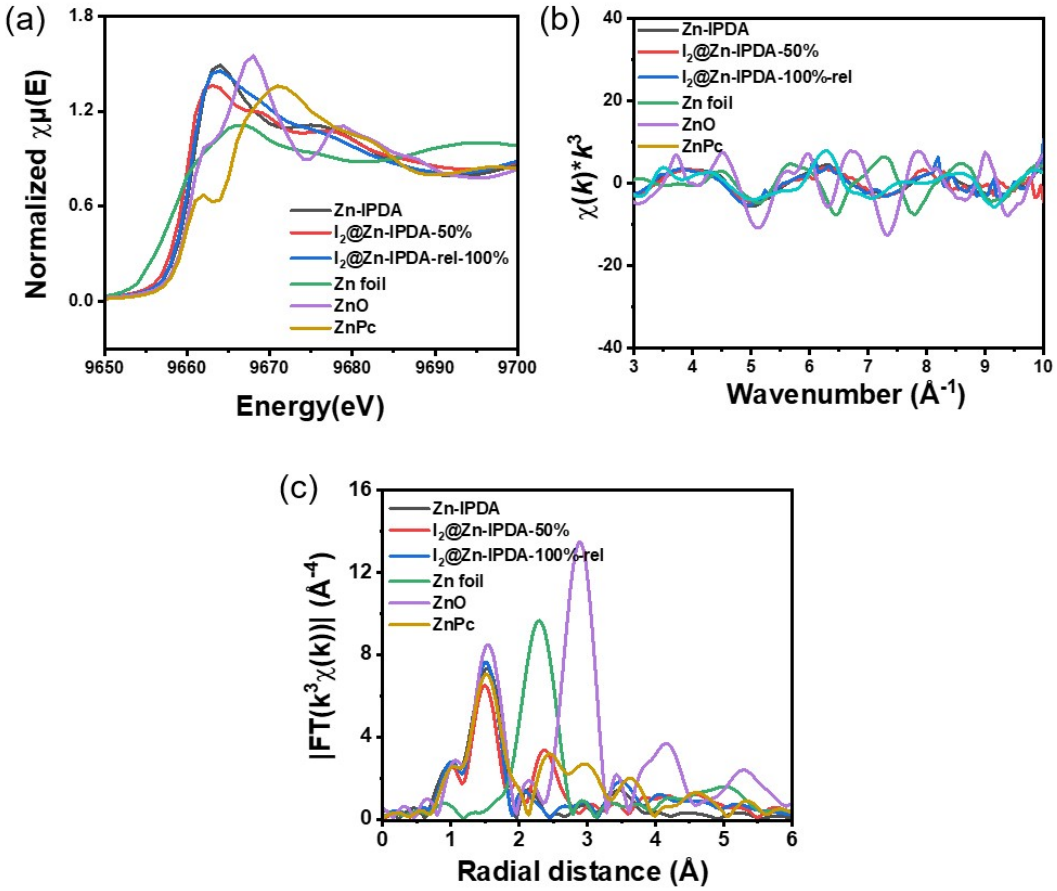

Fig. S13 (a) Zn K-edge XANES spectra of Zn-IPDA, I_2@Zn-IPDA-50%, I_2@Zn-IPDA-100%-rel and reference samples of ZnO, ZnPc, and Zn foil. Fourier transform extended X-ray absorption structure spectra at the Zn K-edge of Zn-IPDA, I_2@Zn-IPDA-50%, I_2@Zn-IPDA-100%-rel reference samples of ZnO, ZnPc, and Zn foil at the (b) K(e) and (c) R(f) spaces.

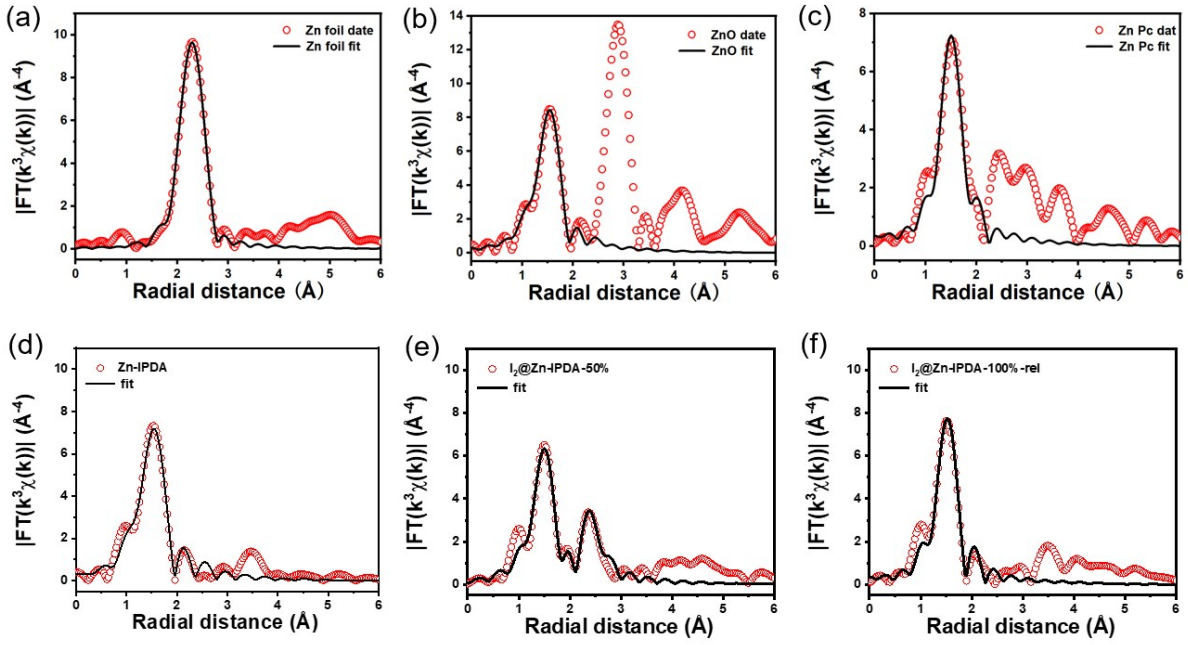

Fig. S14 EXAFS fitting results of FT-EXAFX spectra at the Zn K-edge of (a) Zn foil, (b) ZnO, (c) ZnPc, (d) Zn-IPDA, (e) I_2@Zn-IPDA-50%, and (f) I_2@Zn-IPDA-100%-rel at the R(f) spaces.

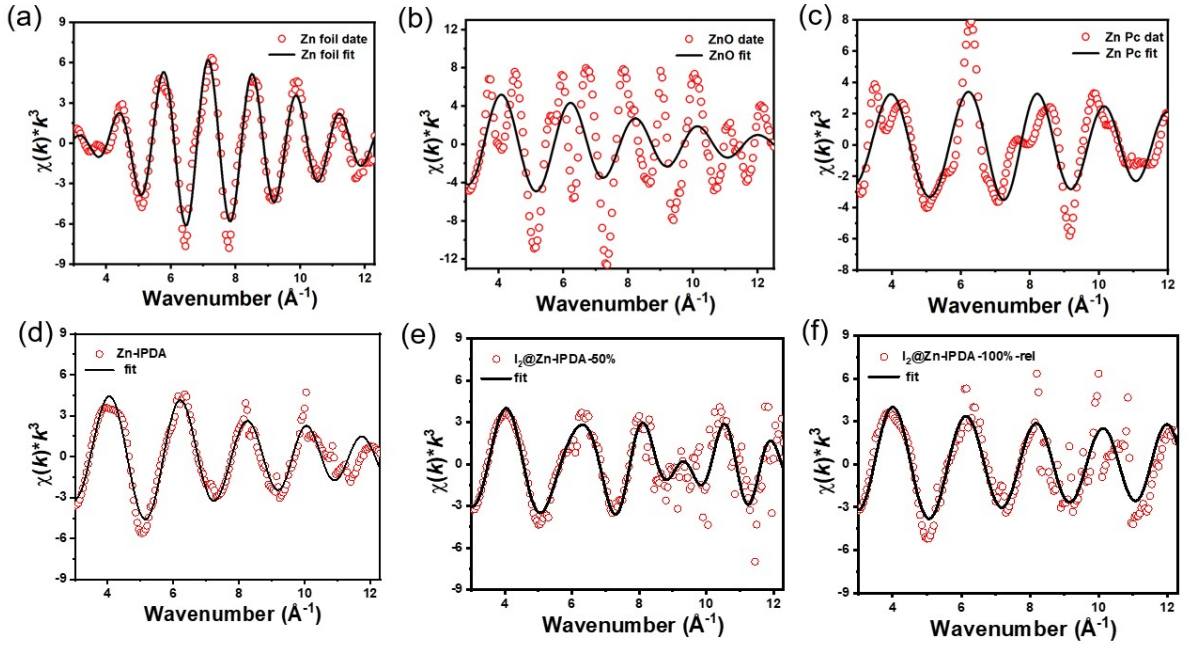

Fig. S15 EXAFS fitting results of FT-EXAFX spectra at the Zn K-edge of (a) Zn foil, (b) ZnO, (c) ZnPc, (d) Zn-IPDA, (e) I_2@Zn-IPDA-50%, and (f) I_2@Zn-IPDA-100%-rel at the K(e) spaces.

.

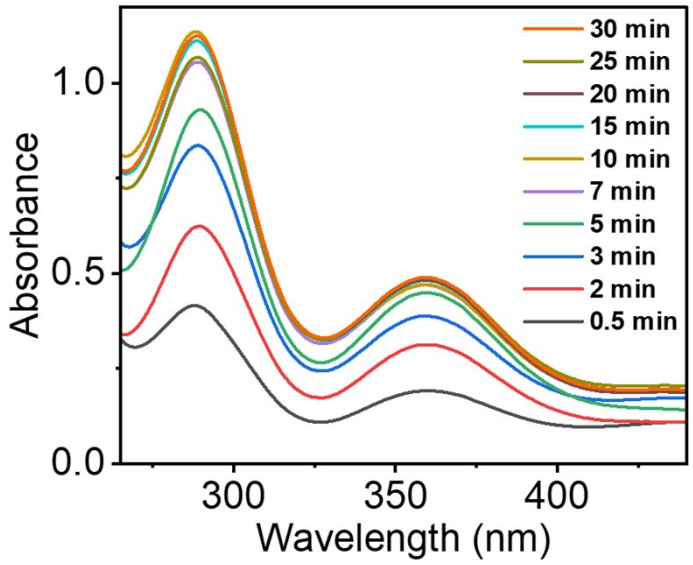

Fig. S16 UV–vis spectra of the ethanol solution by immersing the I_2@Zn-IPDA-100% sample at different times.

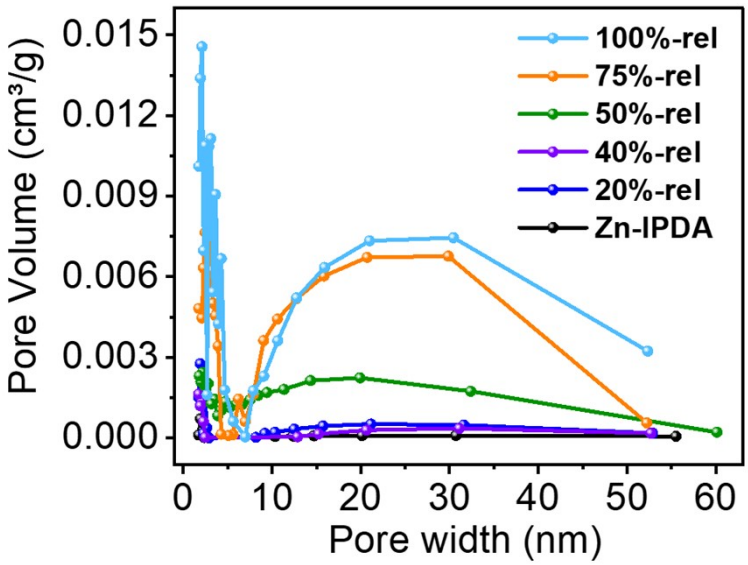

Fig. S17 Pore width distribution calculated from the NLDFT model for Zn-IPDA and I_2@Zn-IPDA-x-rel (x = 20%, 40%, 50%, 75% and 100%).

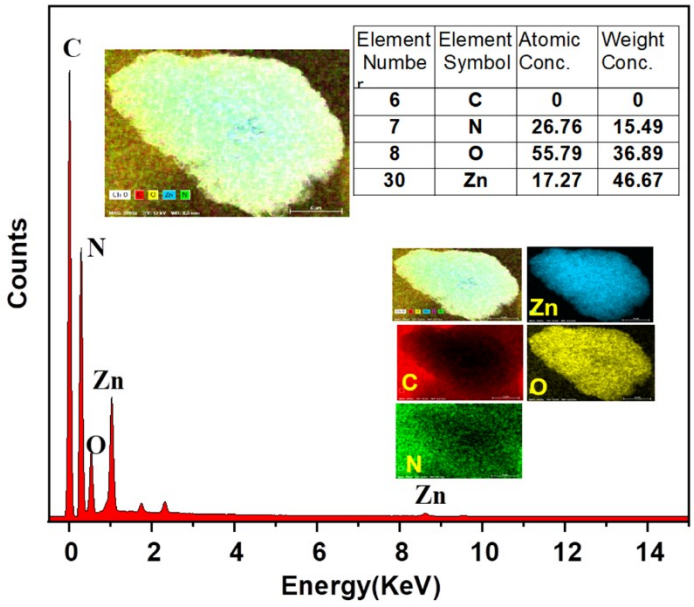

Element Number	Element Symbol	Atomic Conc.	Weight Conc.
6	C	0	0
7	N	26.76	15.49
8	O	55.79	36.89
30	Zn	17.27	46.67

Fig. S18 EDS and mapping of I_2@Zn-IPDA-100%-rel.

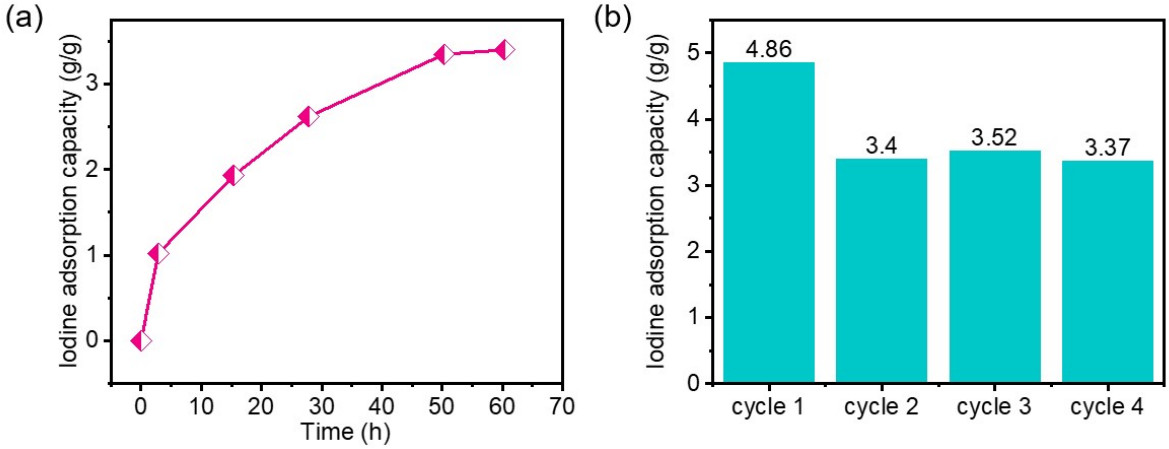

Fig. S19 (a) Time-dependent uptake plots of iodine in I_2@Zn-IPDA-100%-rel at 353 K. (b) Recycling performance of I_2@Zn-IPDA-100%-rel.

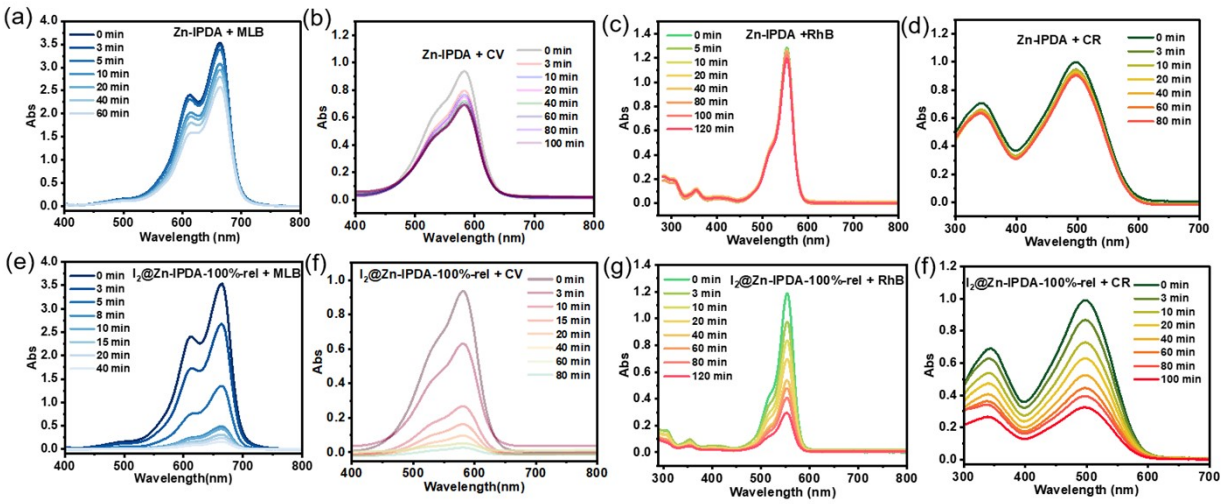

Fig. S20 UV−vis spectra of MLB (a), CV (b), RhB (c), and CR (d) in aqueous solutions at given times during the adsorption process with Zn-IPDA as the host. UV−vis spectra of MLB (e), CV (f), RhB (g), and CR (h) in aqueous solutions at given times during the adsorption process with I_2@Zn-IPDA-100%-rel as the host.

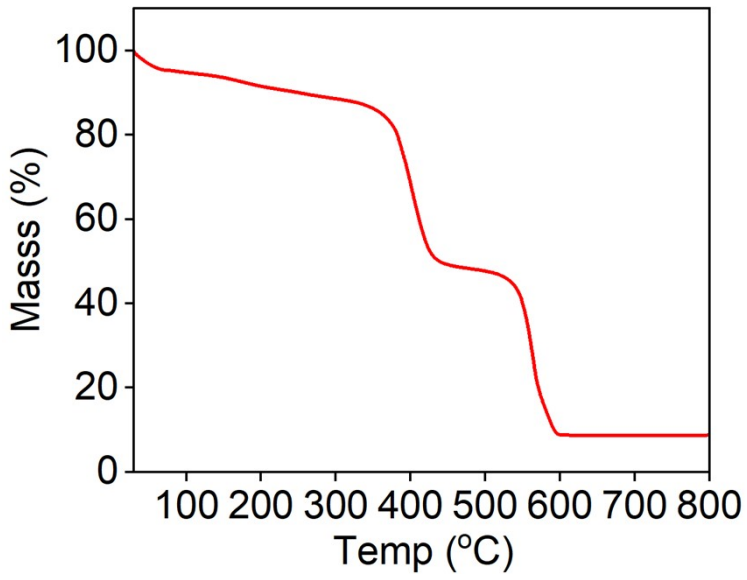

Fig. S21 TG curve of I_2@Zn-IPDA-100%-rel.

Table S1. Crystallographic data and structure refinement summary for Zn-IPDA

Complex	Zn-IPDA
Empirical formula	$C_{84}H_{55}N_9O_{14}Zn_3$
Formula weight	1610.48
Crystal system	monoclinic
Space group	*P*21/n
a/Å	18.0771(8)
b/Å	19.1339(8)
c/Å	24.4666(17)
α/°	90
β/°	97.185(5)
γ/°	90
V/Å^3	8396.2(8)
Z	4
D/g cm^{-3}	1.274
μ/mm^{-1}	1.537
T/K	293(2)
R^a / wR^b	0.07332/0.2019
Total/unique	16616/992

^{a} $R_1 = \Sigma||F_o| - |F_c||/|F_o|$, ^{b} $wR_2 = [\Sigma w(F_o^2 - F_c^2)^2/\Sigma w(F_o^2)^2]^{1/2}$, where $w = 1/[\sigma^2(F_o^2) + (aP)_2 + bP]$. $P = (F_o^2 + 2F_c^2)/3$.

*The refinement results were obtained from squeeze data.

Table S2. Selected bond lengths [Å] and angles [°] for Zn-IPDA

Zn-IPDA			
Zn(1)-N(6)	2.009(4)	Zn(1)-O(2)#1	1.949(4)
Zn(1)-O(6)#2	1.969(4)	Zn(1)-O(13)	1.901(4)
Zn(2)-N(3)#2	2.009(5)	Zn(2)-O(4)	1.947(4)
Zn(2)-O(11)	1.966(4)	Zn(2)-O(13)	1.936(4)
Zn(3)-N(9)#3	2.007(5)	Zn(3)-O(7)	2.006(5)
Zn(3)-O(9)#4	1.988(4)	Zn(3)-O(14)	1.962(8)
O(2)#1-Zn(1)-N(6)	107.19(19)	O(2)#1-Zn(1)-O(6)#2	103.5(2)
O(6)#2-Zn(1)-N(6)	94.18(18)	O(13)-Zn(1)-N(6)	114.73(17)
O(13)-Zn(1)-O(2)#1	117.39(19)	O(13)-Zn(1)-O(6)#2	116.91(19)
O(4)-Zn(2)-N(3)#2	108.4(2)	O(4)-Zn(2)-O(11)	117.34(19)
O(14)-Zn(3)-O(9)#4	106.3(3)	O(11)-Zn(2)-N(3)#2	109.9(2)
O(13)-Zn(2)-N(3)#2	108.62(18)	O(13)-Zn(2)-O(4)	106.31(17)
O(13)-Zn(2)-O(11)	105.87(18)	O(7)-Zn(3)-N(9)#3	104.1(2)

O(9)#4- Zn(3) -N(9)#3	111.54(19)	O(9)#4 -Zn(3) -O(7)	101.65(19)
O(14) -Zn(3) -N(9)#3	114.0(4)	O(14) -Zn(3) -O(7)	119.0(3)

Symmetry transformations used to generate equivalent atoms: #1 -1/2 +x, 3/2 - y, -1/2 + z; #2 -1 + x, y, z; #3 3/2 - x, 3/2 + y, 1/2-z; #4 5/2 -x, 3/2 + y, 1/2 – z.

Table S3. EXAFS fitting parameters at the Zn *K*-edge for various samples.

Sample	Path	N^a	R(Å)^b	σ^2(Å^2)^c	ΔE_0(eV)^d	R factor
Zn foil	Zn-Zn1	6.00*	2.64 (±0.02)	0.0092 (±0.0004)	-2.11 (±0.49)	0.0012
	Zn-Zn2	6.00*	2.74 (±0.02)	0.0077 (±0.0018)	-2.11 (±0.49)	
ZnO	Zn-O	4.00*	1.97 (±0.01)	0.0065 (±0.0008)	3.66 (±1.35)	0.0153
ZnPc	Zn-N	4.00*	1.98 (±0.03)	0.0031 (±0.0009)	4.29 (±1.21)	0.0156
Zn-IPDA	Zn-O	3.15 (±0.17)	1.85 (±0.01)	0.0060 (±0.0028)	-5.54 (±2.69)	0.0077
	Zn-N	1.17 (±0.22)	1.97 (±0.02)	0.0081 (±0.0003)	9.03 (±2.69)	
I_2@ Zn-IPDA	Zn-O	2.39 (±0.35)	1.89 (±0.03)	0.0041 (±0.0025)	8.34 (±2.54)	0.0099
	Zn-N	1.37 (±0.12)	2.01 (±0.01)	0.0071 (±0.0042)	6.63 (±3.45)	
	Zn-I	0.90 (±0.05)	2.78 (±0.02)	0.0030 (±0.0004)	-6.12 (±2.20)	
I_2@Zn-IPDA-rel	Zn-O	2.70 (±0.16)	1.98 (±0.02)	0.0102 (±0.0041)	7.73 (±2.18)	0.0060
	Zn-N	1.09 (±0.04)	2.02 (±0.03)	0.0081 (±0.0014)	6.34 (±2.72)	

^{a}*CN*, coordination number; ^{b}*R*, the distance to the neighboring atom; $^c\sigma^2$, the mean square relative displacement (MSRD); $^d\Delta E_0$, inner potential correction; *R* factor indicates the goodness of fit. $S0^2$ was fixed to 0.70, according to the experimental EXAFS fit of Zn foil by fixing *CN* as the known crystallographic value. * This value was fixed during EXAFS fitting, based on the known structure of Zn. Fitting range: 3.0 ≤ k (/Å) ≤ 12.0 and 1.0 ≤ R (Å) ≤ 3.0 (Zn foil). ; 3.0≤k (/Å) ≤ 11.9 and 1.0 ≤ R (Å) ≤ 2.3(ZnO). ; 3.0 ≤ k (/Å) ≤ 11.1 and 1.0 ≤ R (Å) ≤ 2.4 (ZnPc). ; 3.0 ≤ k (/Å) ≤ 11.0 and 1.0 ≤ R (Å) ≤ 2.8 (Sample 1). ; 3.0 ≤ k (/Å) ≤ 12.0 and 1.0 ≤ R (Å) ≤ 2.8 (Sample 2). ; 3.0≤k (/Å) ≤ 11.1 and 1.0 ≤ R (Å) ≤ 2.4 (Sample 3). A reasonable range of EXAFS fitting parameters: 0.700 < S_0^2 < 1.00; *CN* > 0; σ^2 > 0 Å^2; $|\Delta E_0|$ < 15 eV; *R* factor < 0.02.

REFERENCE

[S1] L. J. Bourhis, O. V. Dolomanov, R. J. Gildea, J. A. K. Howard, H. Puschmann, *Acta Cryst. A* **2015**, *71*, 59.

[S2] G. M. Sheldrick, *Acta Crystallogr., Sect. C: Struct. Chem.* **2015**, *71*, 3.

[S3] A. L. Spek, *J. Appl. Cryst.* **2003**, *36*, 7.

[S4] M. J. Frisch, G. W. Trucks, H. B. Schlegel, et al., Gaussian, Inc., Wallingford CT, **2016**.

[S5] B. Ravel, M. Newville, *J. Synchrotron Radiat.* **2005**, *12*, 537.

[S6] S. I. Zabinsky, J. J. Rehr, A. Ankudinov, R. C. Albers, M. J. Eller, *Phys. Rev. B* **1995**, *52*, 2995.